S-parameter, technimesons, and phase transitions in holographic tachyon DBI models

Mikhail Goykhman and Andrei Parnachev

Institute Lorentz for Theoretical Physics, Leiden University, P. O. Box 9506, 2300 RA Leiden, The Netherlands
(Received 28 November 2012; published 29 January 2013)

We investigate some phenomenological aspects of the holographic models based on the tachyon Dirac-Born-Infeld action in anti–de Sitter space-time. These holographic theories model strongly interacting fermions and feature dynamical mass generation and symmetry breaking. We show that they can be viewed as models of holographic walking technicolor and compute the Peskin-Takeuchi *S* parameter and masses of lightest technimesons for a variety of tachyon potentials. We also investigate the phase structure at finite temperature and charge density. Finally, we comment on the holographic Wilsonian renormalization group in the context of holographic tachyon Dirac-Born-Infeld models.

I. INTRODUCTION AND SUMMARY

Systems of strongly interacting fermions have applications in many realms, including condensed matter (e.g., graphene) and particle physics (e.g., technicolor models). A simple way to introduce interaction between fermions involves adding a quartic term to the Lagrangian of N free fermions, resulting in the Nambu-Jona-Lasinio model (see, e.g., Ref. [1] for a review). In three space-time dimensions, the model is renormalizable to all orders in the $1/N$ expansion: one can take a double scaling limit where the coupling is tuned to the critical value, while the UV cutoff is sent to infinity, keeping the physical mass fixed. Dynamical mass generation at sufficiently large values of the coupling is an important feature, which is believed to happen in other strongly interacting fermion systems.

Unfortunately, one often has to resort to approximate methods to describe the physics in the vicinity of the phase transition from the massless phase to the one with a gap. This is because the transition happens at the intermediate values of the coupling, where both the weak coupling and the strong coupling expansions break down. Nevertheless, such a description is often very useful for phenomenological reasons: for example, the walking technicolor models are precisely of this type, since they stay very close to the putative conformal fixed point for the long renormalization group (RG) time. In Ref. [2], a tachyon dynamics in anti–de Sitter (AdS) space-time was shown to holographically model this type of physics; this has been further studied in Ref. [3] in the context of a particular holographic model based on the tachyon Dirac-Born-Infeld (TDBI) action in AdS. The mass of the tachyon is tuned to the critical value [the Breitenlohner-Freedman (BF) bound], and at the same time the UV cutoff is sent to infinity, so that the physical scale measured, for example, by the meson masses, stays fixed.

In this paper, we study some phenomenological applications of the model proposed in Ref. [3] which, in turn,

was motivated by the holographic description of the dynamics of the D3 and D7 branes intersecting along $2 + 1$ dimensions [4]. We restrict our attention to four space-time dimensions. In the next section, we investigate the phase diagram of the holographic model at finite temperature and charge density. We show that the phase transition at finite temperature between the symmetric and massive phases is generalized into the phase transition line in the temperature-charge density plane. Furthermore, depending on the value of the quartic coefficient in the tachyon potential, the phase transition line can either stay first order, or possess a critical point where the order of the phase transition changes from second to first. This is somewhat similar to the situation with the (conjectural) phase diagram of QCD with massless quarks and constitutes an interesting prediction for the phase diagram of strongly interacting fermions.

In Sec. III, we explore a possibility of using the holographic TDBI model in the context of holographic walking technicolor. We couple the tachyon bilinear to the gauge fields in the adjoint representations of $SU(N_f)_L$ and $SU(N_f)_R$, which contain the electroweak gauge group. (Setting $N_f = 2$ and embedding the electroweak group as $SU(2) \times U(1) \subset SU(2)_L \times SU(2)_R$ constitutes the simplest setup.) Tachyon condensate breaks electroweak symmetry and generates masses for the W and Z bosons, giving rise to a model of holographic walking technicolor. We compute the Peskin-Takeuchi S parameter for a variety of tachyon potentials and observe that it is positive and does not go to zero. In Sec. IV, we compute the masses of the lightest scalar technimesons for a certain family of the tachyon potentials and observe that even though there is no parametrically light "technidilaton," the lowest lying meson can be an order of magnitude lighter than the next one.

We conclude in Sec. V. The Appendix contains an application of the holographic RG to the holographic TDBI model, where a picture for the running of the double-trace coupling, expected from field theoretic considerations, is reproduced.

II. HOLOGRAPHIC TDBI AT FINITE TEMPERATURE AND CHEMICAL POTENTIAL

In this section, we consider the holographic tachyon DBI model at finite temperature and chemical potential. We consider an AdS-Schwarzschild black hole to account for a nonvanishing temperature, and we turn on a background flux of the $U(1)$ gauge potential, which corresponds to the finite density in the dual field theory. We describe the phase with broken conformal symmetry by the dual picture with a nonvanishing tachyon field in the bulk, while the conformally symmetric field theory state corresponds to the identically vanishing tachyon in the bulk. We compute holographically the free energies of both phases and determine the resulting phase diagram.

Perhaps the future development of the results of this section will mostly lie in the realm of condensed matter physics. However, let us make a slight detour and remind the reader of a closely related problem, a phase diagram of QCD at finite temperature and chemical potential. (See, e.g., Refs. [5,6] for recent reviews.) The phase structure of QCD is roughly the following: If the temperature is low and we increase the density, then at some value of the density the system is expected to undergo a first-order phase transition to the states where the hadrons dissociate. At sufficiently large density, the system gets into the color superconducting phase. In this phase, the confined bound state of two quarks goes to the Coulomb bound state in a process similar to Cooper pairing in the microscopic description of a superconductor. Increasing the temperature destroys the Cooper pairing mechanism for the quarks, eventually giving rise to a quark-gluon plasma. This is believed to be a preferred high-temperature state for any value of the chemical potential; however, the phase transition from the hadronic state is first order for larger densities, but second order for smaller densities (for massless quarks). As we will see below, we can observe somewhat similar phase structure for certain TDBI models, though either the orders of first- and second-order phase transitions are interchanged, or we have two critical points at which the order of phase transition changes.

Phase transitions in the holographic tachyon DBI at finite temperature have been studied in Ref. [3], which the reader is encouraged to consult for technical details relevant to the present section.[1] There it has been established that the order of the phase transition is determined by the behavior of the tachyon potential for very small values of T (the tachyon field). In the Berezinskii-Kosterlitz-Thouless (BKT) limit, where the UV cutoff is taken to infinity, with physical observables held fixed, the solution must have a fixed ratio between the two

asymptotics near the boundary of AdS. The value of the coefficient in front of the T^4 term in the tachyon potential determines whether increasing the value of T at the black hole horizon corresponds to smaller or larger temperatures. In the former case, the transition is second order, while in the latter case it is first order. In the following, we repeat this analysis in the presence of finite density.

Consider the finite-temperature AdS_{d+1}-Schwarzschild metric

$$ds^2 = r^2(-F(r)dt^2 + (dx^1)^2 + \cdots + (dx^{d-1})^2) + \frac{dr^2}{r^2F(r)},$$
(2.1)

where $F(r) = 1 - (\frac{r_h}{r})^d$, and turn on nonvanishing flux $\dot{A}_0$. Tachyon DBI action then takes the form

$$S_{\text{TDBI}} = -\int_{r_h}^{\infty} dr \int d^dx r^{d-1} V(T)\sqrt{1 + r^2\dot{T}^2F - \dot{A}_0^2}.$$
(2.2)

From the equation of motion for gauge flux, we obtain

$$\dot{A}_0^2 = \frac{\hat{d}^4(1 + r^2F\dot{T}^2)}{r^{2(d-1)}V^2 + \hat{d}^4},$$
(2.3)

where $\hat{d}(\mu_{\text{ch}}, r_h)$ is a constant of integration. As usual, up to a normalization constant, $\hat{d}^2$ is proportional to the charge density of the system. Due to Eq. (2.3) in the leading order in T, we obtain

$$\mu_{\text{ch}} = \int_{r_h}^{\infty} \frac{dr\hat{d}^2}{\sqrt{\hat{d}^4 + r^{2(d-1)}}}$$

$$= \frac{\hat{d}^2}{(d-2)r_h^{d-2}} {}_2F_1\left(\frac{1}{2}, \frac{d-2}{2(d-1)}, \frac{3d-4}{2(d-1)}, -\frac{\hat{d}^4}{r_h^{2(d-1)}}\right).$$
(2.4)

Plugging Eq. (2.3) into the action [Eq. (2.2)], we arrive at

$$S_{\text{TDBI}} = -\int_{r_h}^{\infty} dr \int d^dx r^{2(d-1)}V^2((1 + r^2F\dot{T}^2)$$

$$\times (r^{2(d-1)}V^2 + \hat{d}^4)^{-1})^{1/2}.$$
(2.5)

We then introduce the dimensionless coordinate $\tilde{r} = r/\hat{d}^{\frac{2}{d-1}}$ and dimensionless temperature $\tilde{r}_h = r_h/\hat{d}^{\frac{2}{d-1}}$. As a result, the action acquires the form

$$S_{\text{TDBI}} = -\hat{d}^{\frac{2d}{d-1}} \int_{\tilde{r}_h}^{\infty} d\tilde{r} \int d^dx \frac{\tilde{r}^{2(d-1)}V^2}{\sqrt{1 + \tilde{r}^{2(d-1)}V^2}}$$

$$\times \sqrt{1 + \tilde{r}^2FT'^2},$$
(2.6)

where $F = 1 - (\tilde{r}_h/)\tilde{r}^d$ and $T' = \partial T/\partial\tilde{r}$.

Let us define the tachyon T value at the horizon, $T_h = T(r_h)$. The equation of motion for the tachyon field, following from the action of Eq. (2.6), is

---

[1]In recent work [7], the phase structure of the holographic model of QCD in the Veneziano limit has been analyzed at finite temperature.

$$\left(\frac{\tilde{r}^{2d}FV^2T'}{\sqrt{(1+\tilde{r}^2FT'^2)(1+\tilde{r}^{2(d-1)}V^2)}}\right)' - \tilde{r}^{2(d-1)}V^2$$

$$\times \frac{2+\tilde{r}^{2(d-1)}V^2}{(1+\tilde{r}^{2(d-1)}V^2)^{3/2}}\sqrt{1+\tilde{r}^2FT'^2}\log V = 0. \quad (2.7)$$

Using Eq. (2.7) and imposing the boundary condition $T(\tilde{r}=\tilde{r}_h)=T_h$, we find

$$T'(\tilde{r}=\tilde{r}_h) = \frac{2+\tilde{r}_h^{2(d-1)}V^2(T_h)}{d\tilde{r}_h(1+\tilde{r}_h^{2(d-1)}V^2(T_h))}\partial_T \log V(T_h). \quad (2.8)$$

When $T \sim T_h \ll 1$ and $m \simeq m_{\mathrm{BF}}^2 = -d^2/4$, we obtain the linearized equation of motion

$$\left(\frac{\tilde{r}^{2d}FT'}{\sqrt{1+\tilde{r}^{2(d-1)}}}\right)' + \frac{d^2\tilde{r}^{2(d-1)}}{4}\frac{2+\tilde{r}^{2(d-1)}}{(1+\tilde{r}^{2(d-1)})^{3/2}}T = 0 \quad (2.9)$$

and boundary conditions

$$T(\tilde{r}=\tilde{r}_h) = T_h, \qquad T'(\tilde{r}=\tilde{r}_h) = -\frac{dT_h}{4\tilde{r}_h}\frac{2+\tilde{r}_h^{2(d-1)}}{1+\tilde{r}_h^{2(d-1)}}. \quad (2.10)$$

Near the boundary $\tilde{r} \to \infty$, the behavior of $T(\tilde{r})$ is given by the equation

$$T'' + \frac{d+1}{\tilde{r}}T' + \frac{d^2}{4\tilde{r}^2}T = 0. \quad (2.11)$$

Let us now specialize to the $d=4$ case. Near-boundary behavior is then described by the equation

$$T'' + \frac{5}{\tilde{r}}T' + \frac{4}{\tilde{r}^2}T = 0, \quad (2.12)$$

which is solved by

$$T(\tilde{r}) \simeq \frac{1}{\tilde{r}^2}(c_1\log\tilde{r}+c_2) \Rightarrow T(r) = \frac{1}{r^2}\left(c_1\log\frac{r}{\hat{d}^{2/3}}+c_2\right). \quad (2.13)$$

Let us denote

$$g = \hat{d}^{2/3}. \quad (2.14)$$

The constants c_1 and c_2 can be determined by solving the equation of motion [Eq. (2.7)] numerically. If we consider instead the linearized equation (2.9) in the BKT limit with the boundary conditions of Eq. (2.10), we obtain c_2/c_1, which is a function of $\tilde{r}_h = r_h/g$. In the case of vanishing temperature and vanishing chemical potential, the near-boundary behavior of tachyon field is given by

$$T(r) = \frac{1}{r^2}\left(C_1\log\frac{r}{\mu}+C_2\right). \quad (2.15)$$

Clearly, it must be the same as Eq. (2.13). Matching these equations, we obtain

$$\frac{g}{\mu} = C_0\exp\left(\Xi\left(\frac{r_h/\mu}{g/\mu}\right)\right), \quad (2.16)$$

where we have denoted $C_0 = e^{-C_2/C_1}$ and $\Xi = c_2/c_1$. Equation (2.16) can be solved numerically, which gives critical values of temperature r_h and g measured in units of μ. The result appears in Fig. 1. We have checked that when $\hat{d}=0$, the critical temperature is equal to $2C_0$, which is a correct limiting value [3].

To determine which state in the canonical ensemble is preferred, we need to compare the free energies. Similarly to Ref. [3], we focus on the near-critical region, where the tachyon field is either vanishing or small. The difference in free energy between nonvanishing and vanishing tachyon phases is given by

$$\mathcal{F}(r_h,\hat{d}) = S_{\mathrm{TDBI}}(T \equiv 0) - S_{\mathrm{TDBI}}(T), \quad (2.17)$$

where the last term on the right-hand side is evaluated on the solution, satisfying the $T(r=r_h)=T_h$ boundary condition. Due to $V(0)=1$, one obtains, using Eq. (2.6),

$$\mathcal{F}(r_h,\hat{d}) = \hat{d}^{8/3}\int_h^\infty d\tilde{r}\int d^4x\,\tilde{r}^6$$

$$\times \left(\frac{V^2}{\sqrt{1+\tilde{r}^6\tilde{r}V^2}}\sqrt{1+\tilde{r}^2FT'^2} - \frac{1}{\sqrt{1+\tilde{r}^6}}\right). \quad (2.18)$$

We will need the form of the tachyon potential near $T=0$:

$$V(T) = 1 + \frac{1}{2}m^2T^2 + \frac{a}{4}T^4 + \cdots, \quad (2.19)$$

where $m^2 \simeq m_{\mathrm{BF}}^2 = -4$, and a is the coefficient of the quartic term which, as explained in Ref. [3], determines the order of the phase transition in the case of vanishing
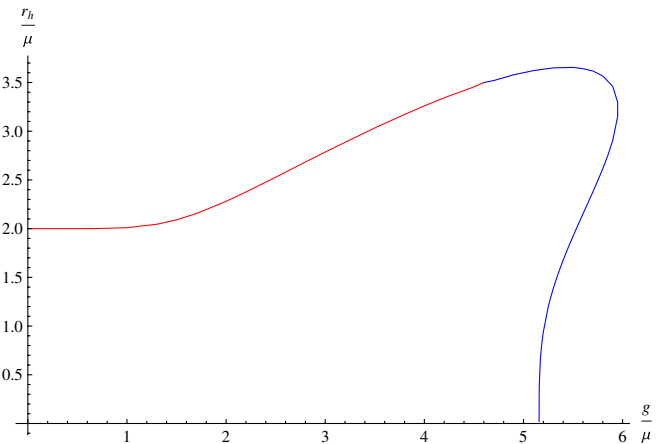

FIG. 1 (color online). Phase diagram for conformal phase transition in the $(g/\mu, r_h/\mu)$ plane. The order of the phase transition changes at the point $\tilde{r}_h \equiv r_h/g = 0.75$. The blue part of the curve $(g/\mu > 4.6)$ describes the second-order phase transition, and red part of the curve $(g/\mu < 4.6)$ describes the first-order phase transition.

density. Below we will see that at finite density the situation is more subtle, and the first-order phase transition line can join the second-order phase transition line at a critical point, provided the value of a is chosen accordingly.

In the BKT limit, we have $T \sim T_h \ll 1$ and $m^2 = m_{BF}^2 = -4$. We compute Eq. (2.18) up to the fourth order in T_h:

$$\mathcal{F}(r_h, \hat{d}) = \mathcal{F}_2(r_h, \hat{d}) + \mathcal{F}_4(r_h, \hat{d}) + \cdots, \qquad (2.20)$$

where

$$\mathcal{F}_2 = \hat{d}^{8/3} \int_h^\infty d\tilde{r} \int d^4x \frac{1}{2\sqrt{1+\tilde{r}^6}}\left(\tilde{r}^8 F T'^2 - 4\tilde{r}^6 \frac{2+\tilde{r}^6}{1+\tilde{r}^6} T^2\right),$$

$$\mathcal{F}_4 = -\hat{d}^{8/3} \int_h^\infty d\tilde{r} \int d^4x \frac{\tilde{r}^6}{8(1+\tilde{r}^6)^{5/2}}(F^2 T'^4 \tilde{r}^4 (1+\tilde{r}^6)^2$$
$$+ 8F\tilde{r}^2 T^2 T'^2(1+\tilde{r}^6)(2+\tilde{r}^6) + 2T^4(8(\tilde{r}^6-2)$$
$$- a(1+\tilde{r}^6)(2+\tilde{r}^6))). \qquad (2.21)$$

The quadratic terms vanish on shell, up to the boundary term, which also vanishes, because

$$F(\tilde{r} = \tilde{r}_h) = 0, \qquad T(\tilde{r} = \infty) = 0. \qquad (2.22)$$

We solve numerically Eq. (2.9) with the boundary conditions in Eq. (2.10), for each particular $\tilde{r}_h = r_h/g$. This gives us $T = T_1$, which is a solution of the first order in T_h. The first correction to this solution is obtained when we take into account terms in the action for T that are quartic in T_h, and therefore the corrected solution is $T = T_1 + T_3$, where T_3 is of the third order in T_h. Therefore, we need to compute in the leading order

$$\mathcal{F}(T_1 + T_3) = \mathcal{F}_2(T_1 + T_3) + \mathcal{F}_4(T_1 + T_3). \qquad (2.23)$$

For brevity, let us rewrite Eq. (2.21) as

$$\mathcal{F}_2 = \int dr[\alpha(r)T^2 + \beta(r)T'^2],$$
$$\mathcal{F}_4 = \int dr[a(r)T^4 + b(r)T^2T'^2 + c(r)T'^4]. \qquad (2.24)$$

Let us use integration by parts to bring $\mathcal{F}_{2,4}$ to the form

$$\mathcal{F}_2 = \int dr T[\alpha T - (\beta T')'] \equiv \int dr T P_1,$$
$$\mathcal{F}_4 = \int dr T \left[aT^3 + \frac{b}{2}TT'^2 - \left(\frac{b}{2}T'T^2\right)' - (cT'^3)'\right]$$
$$\equiv \int dr T P_3, \qquad (2.25)$$

where $P_{1,3}$ are polynomials of T, T', T'' of the degree specified by the subscript. From the variation

$$\delta\mathcal{F} = 2\int dr \delta T[\alpha T - (\beta T')']$$
$$+ 4\int dr \delta T\left[aT^3 + \frac{b}{2}TT'^2 - \left(\frac{b}{2}T'T^2\right)' - (cT'^3)'\right], \qquad (2.26)$$

we obtain the equation of motion

$$2P_1(T_1 + T_3) + 4P_3(T_1 + T_3) = 0, \qquad (2.27)$$

which we can solve perturbatively as

$$P_1(T_1) = 0, \qquad P_1(T_3) + 2P_3(T_1) = 0. \qquad (2.28)$$

Using these equations in the expansion of Eq. (2.23),

$$\mathcal{F} = \int dr(T_1 + T_3)P_1(T_1 + T_3) + (T_1 + T_3)P_3(T_1 + T_3)$$
$$= \int dr T_1 P_1(T_3) + T_3 P_1(T_1) + T_1 P_3(T_1) + \cdots, \qquad (2.29)$$

we obtain

$$\mathcal{F}(T) \simeq -\int dr T_1 P_3(T_1) = -\mathcal{F}_4(T_1). \qquad (2.30)$$

We then evaluate the quartic terms, $\mathcal{F}_4(\hat{d}, a)$, on the numerically found solution T_1. Equation $\mathcal{F}_4(\tilde{r}_h, a) = 0$ gives values of ratio $r_h/g = \tilde{r}_h$ for each particular a at which the order of the phase transition changes. This equation is valid only for those values of r_h and $\hat{d}$ which are close to critical ones. We solve this equation numerically for each particular value of the parameter a; that is, we find $\tilde{r}_h^{(c)}(a)$. The result is plotted in Fig. 2. Notice that when $\hat{d}$ is sent to zero, $\tilde{r}_h$ goes to infinity, and the special
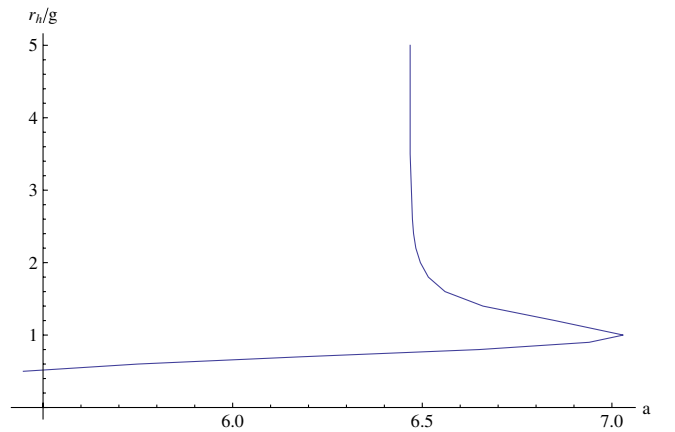

FIG. 2 (color online). The ratio $\tilde{r}_h = r_h/g$ at which the order of phase transition changes, as a function of the UV parameter a. It is determined by the sign of $\mathcal{F}_4$ in the conformal symmetry broken phase. On the left side of the curve, $\mathcal{F}_4 < 0$, and the phase transition is of the first order; on the right side, $\mathcal{F}_4 > 0$, and the phase transition is of the second order.

value $a \simeq 6.47$ becomes the same as in the case of vanishing chemical potential [3]. Also notice that when $6.47 \leq a \leq 7.03$, there are two points $\tilde{r}_h$ at which the order of phase transition changes.

In Fig. 1, we have taken $a = 6.41$, for which the phase transition is the second-order one for $\frac{r_h}{g} < 0.75$ and the first-order one for $\frac{r_h}{g} > 0.75$. This corresponds to the blue ($g/\mu > 4.6$) and red ($g/\mu < 4.6$) parts, respectively, of the phase transition curve in Fig. 1.[2]

The other option is to take the value of a at which we have two critical points where the order of phase transition changes. Then, for the temperature below some critical value, $\tilde{r}_h^{(c)} < r_h^{(c,1)}$, we have a second-order phase transition; for $\tilde{r}_h^{(c,1)} < \tilde{r}_h^{(c)} < \tilde{r}_h^{(c,2)}$, we have a first-order order phase transition; and finally, for $\tilde{r}_h^{(c)} > \tilde{r}_h^{(c,2)}$, we have a second-order phase transition. The critical point $\tilde{r}_h^{(c,2)}$ therefore resembles the one in the QCD phase diagram.

As emphasized in Ref. [3], the behavior of the free energy for small values of the tachyon condensate determines the order of the phase transition, provided the phase diagram has a simple form. This was the case in all examples studied in Ref. [3]. We believe this remains true once the finite density is turned on, but to show this, some further numerical work is necessary.

III. *S* PARAMETER

A. Review of technicolor and *S*, *T*, *U* parameters

Consider the system of two techniquark matter fields $(\tilde{u}, \tilde{d})$ with color charges, transforming in fundamental representation of the gauge group $SU(N_c)$. Quark fields are coupled to gauge fields in the adjoint representation of the gauge group. In the ultraviolet regime, these quarks are massless, and therefore the system possesses the $SU(2)_L \times SU(2)_R$ chiral symmetry. Therefore, we can couple the doublet of left quarks $Q = (\tilde{u}_L, \tilde{d}_L)$ to bosons of the weak gauge group $SU(2)_L$, leaving two right quarks, $\tilde{u}_R$ and $\tilde{d}_R$, in the singlet representation sector of the weak gauge transformations. We also give each quark field the hypercharge Y, characterizing its representation under the action of the $U(1)_Y$ gauge group.

We look at two quarks as a set of strongly interacting fermionic fields of the physics beyond the Standard Model. At some energy scale, due to the strong interaction, these quarks may form a chiral condensate, breaking the chiral symmetry down to $SU(2)_{\text{diag}}$.[3] In the vacuum, with

spontaneously broken chiral symmetry, the two quarks acquire a mass. In the technicolor models, the phenomenon of chiral symmetry breaking via techniquark condensation is used to explain the spontaneous electroweak symmetry breaking, realized therefore as a dynamical symmetry breaking. Furthermore, the extended technicolor models combine these two techniquarks with Standard Model (SM) matter fields in some specific multiplets in such a way that the condensation of techniquarks gives masses to SM matter fields. In the simplest technicolor models, such quartic fermionic terms, generated at high-scale Λ_{ETC}, lead to flavor-changing neutral current matrix elements that are way above experimental bounds. A walking technicolor model, where the system spends a long RG time in the vicinity of a putative RG fixed point and the anomalous dimension of the technimeson condensate $\gamma \simeq 1$, has been proposed to alleviate this problem. (See Ref. [10] for a recent review of walking technicolor and references therein.) The theory is necessarily strongly coupled, and it is natural to use holography in this context.

To create a possibility for experimental tests of theories describing physics beyond the Standard Model, Peskin and Takeuchi [11,12] introduced dimensionless parameters S, T, U, measuring the impact of a hidden sector of heavy beyond-SM fundamental matter fields coupled to electroweak gauge bosons. They argued (following Ref. [13]) that the most important impact arises from oblique corrections: vacuum polarization diagrams, which renormalize gauge boson propagators. Peskin-Takeuchi parameters are expressed via these vacuum polarization amplitudes, and we will review their argument in greater detail below. For each beyond-SM theory, we therefore may compute S, T, U parameters and see whether the results lie within the boundaries set by the deviation of experimental data from Standard Model predictions.

The quantum corrections of matter fields to the propagators of the SM gauge fields come from the vacuum polarization amplitudes

$$\int d^4x \, e^{iq \cdot x} \langle J_a^\mu(x) J_b^\nu(0) \rangle = -i \left(g^{\mu\nu} - \frac{q^\mu q^\nu}{q^2} \right) \Pi_{ab}(q^2),$$

(3.1)

where a, $b = 1, 2, 3, Q$, and we are assuming mostly plus signature of the metric. The expression (3.1) should be computed for the matter fields of the SM and for the hidden matter sector of the beyond-SM physics. For weak currents J_i, where $i = 1, 2$; weak isospin current J_3; and electromagnetic current J_Q; we have the vacuum polarization amplitudes

$$\Pi_{11}, \ \Pi_{22}, \ \Pi_{33}, \ \Pi_{3Q}, \ \Pi_{QQ}. \qquad (3.2)$$

If we know these amplitudes, then using the expression for the electroweak interaction Lagrangian,

---

[2]One may use the top-down approach based on the $D3$–$D7$ system to derive the phase diagram of $N = 4$ super-Yang-Mills coupled to $N = 2$ matter at finite temperature and chemical potential. It also exhibits the phase transition of the second order at small temperatures. See Ref. [8] for a recent discussion.

[3]It was shown in Ref. [9] that under general assumptions in large-N_c chromodynamics, the chiral symmetry breaks spontaneously.

$$L = \frac{e}{\sqrt{2}s}(W_\mu^+ J_+^\mu + W_\mu^- J_-^\mu) + \frac{e}{sc}Z_\mu(J_3^\mu - s^2 J_Q^\mu) + eA_\mu J_Q^\mu, \tag{3.3}$$

we can obtain one particle irreducible self-energies for the electroweak gauge bosons, and one particle irreducible mixing for the Z boson and photon,

$$\Pi_{AA} = e^2 \Pi_{QQ}, \quad \Pi_{ZA} = \frac{e^2}{sc}(\Pi_{3Q} - s^2 \Pi_{QQ}), \dots \tag{3.4}$$

Then, with the help of Schwinger-Dyson equations, we can derive full quantum propagators for the electroweak gauge fields.

Now, in the interaction Lagrangian [Eq. (3.3)], we have the parameters e and

$$s^2 \equiv \sin^2\theta_W = 1 - \frac{m_W^2}{m_Z^2}. \tag{3.5}$$

Quantum corrections due to the vacuum polarization amplitudes boil down to the renormalization of these parameters:

$$e_\star^2(q^2) \equiv \frac{e^2}{1 - e^2 \Pi_{QQ}(q^2)}, \tag{3.6}$$

$$s_\star^2(q^2) \equiv s^2 - sc \frac{\Pi_{ZA}(q^2)}{q^2 - \Pi_{AA}(q^2)}. \tag{3.7}$$

Then, the renormalized parameter $s_\star$ enters the measured left-right Z-decay asymmetry,

$$A_{\mathrm{LR}}(q^2) = \frac{2(1 - 4s_\star^2)}{1 + (1 - 4s_\star^2)^2}, \tag{3.8}$$

and therefore the renormalization of the gauge field propagators (coming mainly as oblique corrections due to loops of heavy fermions) can be measured experimentally.

Let us also define θ_0 as

$$\sin(2\theta_0) = \sqrt{\frac{4\pi\alpha_{\star,0}(m_Z^2)}{\sqrt{2}G_F m_Z^2}}. \tag{3.9}$$

Here m_Z and G_F are experimentally measured. And $\alpha_{\star,0}(m_Z^2)$ is a running electromagnetic coupling, which is computed due to known physics up to the $q^2 = m_Z^2$ scale. The running starts from the measured $\alpha(q^2 = 0) = e^2/(4\pi)$.

The renormalization comes from SM and from physics beyond the SM. In the SM, the most important contribution comes from t-quark loops (see, e.g., Ref. [14], Chap. 21):

$$s^2 - s_\star^2 = -\frac{3\alpha c^2}{16\pi s^2}\frac{m_t^2}{m_Z^2}, \tag{3.10}$$

$$s_\star^2 - s_0^2 = -\frac{3\alpha}{16\pi(c^2 - s^2)}\frac{m_t^2}{m_Z^2}. \tag{3.11}$$

Let us now describe quantum corrections due to vacuum polarization diagrams of beyond-SM physics. First of all, for heavy fermions, we can expand the vacuum polarization amplitudes around $q^2 = 0$:

$$\Pi_{QQ}(q^2) = q^2 \Pi'_{QQ}(0), \quad \Pi_{3Q}(q^2) = q^2 \Pi'_{3Q}(q^2), \tag{3.12}$$

$$\Pi_{33}(q^2) = \Pi_{33}(0) + q^2 \Pi'_{33}(0), \tag{3.13}$$

$$\Pi_{11}(q^2) = \Pi_{11}(0) + q^2 \Pi'_{11}(0), \tag{3.14}$$

where the prime denotes differentiation with respect to q^2, and we have made use of the fact that the Ward identity for the electromagnetic field ensures that $\Pi_{QQ}(0) = 0$ and $\Pi_{3Q}(0) = 0$. Also, we have $\Pi_{11} = \Pi_{22}$. We therefore have six parameters defining the vacuum polarization amplitudes of heavy fermions. We make a renormalization, fixing the values of three well-measured parameters, which are α, G_F, and m_Z. The three parameters which are left are free of UV divergencies, and we combine these into

$$\alpha S = 4e^2(\Pi'_{33}(0) - \Pi'_{3Q}(0)), \tag{3.15}$$

$$\alpha T = \frac{e^2}{s^2 c^2 m_Z^2}(\Pi_{11}(0) - \Pi_{33}(0)), \tag{3.16}$$

$$\alpha U = 4e^2(\Pi'_{11}(0) - \Pi'_{33}(0)). \tag{3.17}$$

In addition to SM corrections [Eqs. (3.10) and (3.11)], we can write down the contribution of beyond-SM physics via these parameters:

$$\frac{m_W^2}{m_Z^2} - c_0^2 = \frac{\alpha c^2}{c^2 - s^2}\left(-\frac{1}{2}S + c^2 T + \frac{c^2 - s^2}{4s^2}U\right), \tag{3.18}$$

$$s_\star^2 - s_0^2 = \frac{\alpha}{c^2 - s^2}\left(\frac{1}{4}S - s^2 c^2 T\right). \tag{3.19}$$

Thus, we have explicitly constructed a set of experimentally measured quantities, quantum corrections to which may be separately computed from the SM [Eqs. (3.10) and (3.11)], and from a hidden sector [Eqs. (3.18) and (3.19)], with the latter being expressed via Peskin-Takeuchi parameters.

Let us use vector and axial-vector isospin currents,

$$J_V^\mu = \bar{\psi}\gamma^\mu\tau_3\psi, \qquad J_A^\mu = \bar{\psi}\gamma^\mu\gamma^5\tau_3\psi, \tag{3.20}$$

to express the left isospin current as

$$J_3^\mu = \frac{1}{2}(J_V^\mu - J_A^\mu). \tag{3.21}$$

Consider also the electromagnetic current, expressed via isospin and hypercharge currents in a usual way,

$$J_Q^\mu = J_V^\mu + \frac{1}{2}J_Y^\mu. \tag{3.22}$$

Assuming the conservation of parity by technicolor interactions, we can express the isospin current correlator via vector and axial vector isospin correlators: $\Pi_{33} = \frac{1}{4} \times (\Pi_{VV} + \Pi_{AA})$. We also note that due to isospin conservation, $\langle J_3 J_Y \rangle = 0$ (otherwise, in technicolor models, there would have been a preferred isospin direction), and we obtain $\Pi_{3Q} = \frac{1}{2}\Pi_{VV}$. Therefore,

$$S = -4\pi(\Pi'_{VV}(q^2) - \Pi'_{AA}(q^2))|_{q^2=0}. \quad (3.23)$$

The holographic tachyon DBI was introduced in Ref. [3] to describe a system of strongly interacting fermions, which can be made into the walking technicolor theory. However, for the purpose of computing the *S* parameter and technimeson masses, we do not even need to specify that the holographic TDBI model describes strongly interacting fermions. Instead, it is sufficient to treat the holographic model as a black box, which produces two-point functions for the vector and axial currents and features spontaneous breaking of the axial symmetry. Then, these currents are coupled to the SM gauge fields to produce spontaneous symmetry breaking of the electroweak gauge group. The resulting contribution to the *S* parameter is given by Eq. (3.23) and is computed below.

B. Computation of the *S* parameter from the tachyon DBI action

As pointed out above, the holographic tachyon DBI theory provides a natural model of the walking technicolor scenario. The important feature of the holographic approach is that we can isolate the impact of the beyond-SM sector of the theory. For this purpose, we just have to consider a corresponding set of fields in the bulk and study its classical dynamics.[4]

We need to construct a dual to a strongly interacting theory with the $SU(2)_L \times SU(2)_R$ global symmetry in the UV. The global currents $j_\mu^{(L)}$ and $j_\mu^{(R)}$ give rise to the bulk fields $A_M^{(L,R)}$, living in adjoint of $SU(2)_{L,R}$, with the gauge transformations

$$\begin{aligned} A_M^{(L)} &\to U_L A_M^{(L)} U_L^\dagger + i\partial_M U_L U_L^\dagger, \\ A_M^{(R)} &\to U_R A_M^{(R)} U_R^\dagger + i\partial_M U_R U_R^\dagger. \end{aligned} \quad (3.24)$$

The tachyon field $T(r, x)$ lives in the bifundamental of $SU(2)_L \times SU(2)_R$; i.e., its gauge transformations are given by

$$T \to U_L T U_R^\dagger. \quad (3.25)$$

Tachyon action with $SU(2)_L \times SU(2)_R$ local symmetry in the bulk is then

[4]Previous work dedicated to holographic technicolor and *S* parameter includes Refs. [15–46]; see also Refs. [47–53] for recent related work.

$$S = -\int d^4x\, dr\, \mathrm{Tr} V(|T|)(\sqrt{-G^{(L)}} + \sqrt{-G^{(R)}}), \quad (3.26)$$

where

$$G_{MN}^{(R)} = G_{MN} + F_{MN}^{(R)}, \qquad G_{MN} = g_{MN} + (D_{(M}T)^\dagger D_{N)}T,$$
$$G^{(R)} = \det G_{MN}^{(R)}, \quad (3.27)$$

and similar for the left fields; and the covariant derivative of the tachyon field is given by

$$D_M T = \partial_M T + i A_M^{(L)} T - i T A_M^{(R)}. \quad (3.28)$$

Similar actions for the tachyon have been introduced in Ref. [54].

We have $A_M^{(L,R)} = (A_r^{(L,R)}, A_\mu^{(L,R)})$, and we partly fix the gauge symmetry, setting

$$A_r^{(L)} = 0, \qquad A_r^{(R)} = 0. \quad (3.29)$$

Let us introduce gauge fields in the bulk, dual to vector and axial currents on the boundary:

$$A_M^{(L)} = \frac{1}{2}(V_M - A_M), \qquad A_M^{(R)} = \frac{1}{2}(V_M + A_M). \quad (3.30)$$

Suppose we have a background tachyon field $T(r) = \langle T(r) \rangle I$, with the real-valued vacuum average $\langle T(r) \rangle = T_0(r)$, satisfying the equation of motion at vanishing gauge fields,

$$\frac{d}{dr}\left(\frac{r^5 \dot{T}_0}{\sqrt{1 + r^2 \dot{T}_0^2}}\right) = \frac{r^3 \partial_T \log V(T_0)}{\sqrt{1 + r^2 \dot{T}_0^2}}. \quad (3.31)$$

Such a background tachyon field breaks the symmetry down to $SU(2)_{\mathrm{diag}}$, which means that $U_L = U_R$. Its nonzero covariant derivative components, due to the gauge choice [Eq. (3.29)] and definition [Eq. (3.30)] are

$$D_r T = \dot{T}_0 I, \qquad D_\mu T = -i A_\mu T_0. \quad (3.32)$$

(The fact that T couples only to the axial field A means that axial symmetry is broken.)

In what follows, we consider the case of just one flavor of quark field. The results can be generalized to an arbitrary number of flavors, because for the holographic computation of two-point functions, higher-order non-Abelian terms in gauge field Lagrangians do not play any role. We therefore have

$$G_{MN} = g_{MN} + \partial_M T_0 \partial_N T_0 + A_M A_N T_0^2. \quad (3.33)$$

Let us denote for brevity

$$\begin{aligned} \mathcal{G}_{MN} &= g_{MN} + \partial_M T_0 \partial_N T_0 \\ &= \mathrm{diag}\left(-r^2, r^2, r^2, r^2, \frac{1 + r^2 \dot{T}_0^2}{r^2}\right), \end{aligned} \quad (3.34)$$

and let us write down an inverse matrix to Eq. (3.34):

$$\mathcal{M}^{MN} \equiv (\mathcal{G}^{-1})^{MN} = \text{diag}\left(-\frac{1}{r^2}, \frac{1}{r^2}, \frac{1}{r^2}, \frac{1}{r^2}, \frac{r^2}{1 + r^2\dot{T}_0^2}\right).$$
(3.35)

We also denote

$$\sqrt{-G} = \sqrt{-\det\|G_{MN}\|},$$
$$\sqrt{-G_0} = \sqrt{-\det\|\mathcal{G}_{MN}\|} = r^3\sqrt{1 + r^2\dot{T}_0^2},$$
(3.36)

$$K_{MN} = G_{MN} - \mathcal{G}_{MN} = A_M A_N T_0^2.$$
(3.37)

Up to the second order in A, we expand

$$\sqrt{-G} = \sqrt{-G_0}\exp\left(\frac{1}{2}\,\text{tr}\log(1 + \mathcal{M}K)\right)$$
$$= r^3\sqrt{1 + r^2\dot{T}_0^2}\left(1 + \frac{T_0^2}{2r^2}\eta^{\mu\nu}A_\mu A_\nu\right).$$
(3.38)

Expanding the action of Eq. (3.26) up to the second power of gauge fields, and replacing left and right gauge fields with vectors and axials, we get

$$S = -\int d^4x dr V(T_0)\sqrt{-G}\left(2 + \frac{1}{4}(G^{-1})^{M_1 M_2}(G^{-1})^{N_1 N_2}\right.$$
$$\left. \times (F^{(L)}_{M_1 N_1}F^{(L)}_{M_2 N_2} + F^{(R)}_{M_1 N_1}F^{(R)}_{M_2 N_2})\right)$$
$$= -\int d^4x dr V(T_0)r^3\sqrt{1 + r^2\dot{T}_0^2}\left[2 + \frac{T_0^2}{r^2}\eta^{\mu\nu}A_\mu A_\nu\right.$$
$$\left. + \frac{1}{8}\mathcal{M}^{M_1 M_2}\mathcal{M}^{N_1 N_2}(F^{(V)}_{M_1 N_1}F^{(V)}_{M_2 N_2} + F^{(A)}_{M_1 N_1}F^{(A)}_{M_2 N_2})\right].$$
(3.39)

Using Eq. (3.35) for $\mathcal{M}$, and throwing away what is independent of gauge fields, we proceed to

$$S = -\int d^4x dr V(T_0)r^3\sqrt{1 + r^2\dot{T}_0^2}$$
$$\times \left[\frac{1}{4(1 + r^2\dot{T}_0^2)}\eta^{\mu\nu}(\dot{V}_\mu \dot{V}_\nu + \dot{A}_\mu \dot{A}_\nu)\right.$$
$$\left. + \frac{1}{8r^4}\eta^{\mu\nu}\eta^{\lambda\rho}(F^{(V)}_{\mu\lambda}F^{(V)}_{\nu\rho} + F^{(A)}_{\mu\lambda}F^{(A)}_{\nu\rho}) + \frac{T_0^2}{r^2}\eta^{\mu\nu}A_\mu A_\nu\right].$$
(3.40)

We now go to momentum representation,

$$V_\mu(x, r) = \int \frac{d^4q}{(2\pi)^2}V_\mu(q, r)e^{-iq_\lambda x^\lambda},$$
$$A_\mu(x, r) = \int \frac{d^4q}{(2\pi)^2}A_\mu(q, r)e^{-iq_\lambda x^\lambda},$$
(3.41)

which results in

$$S = -\int d^4q dr V(T_0)r^3\sqrt{1 + r^2\dot{T}_0^2}$$
$$\times \left[\frac{1}{4(1 + r^2\dot{T}_0^2)}\eta^{\mu\nu}(\dot{V}_\mu \dot{V}_\nu + \dot{A}_\mu \dot{A}_\nu)\right.$$
$$+ \frac{q^2}{4r^4}\left(V_\mu V_\nu\left(\eta^{\mu\nu} - \frac{q^\mu q^\nu}{q^2}\right)\right.$$
$$\left.\left. + A_\mu A_\nu\left(\eta^{\mu\nu}\left(1 + \frac{4T_0^2 r^2}{q^2}\right) - \frac{q^\mu q^\nu}{q^2}\right)\right)\right], \quad (3.42)$$

where all squared gauge fields are just a short notation for q-mode and $-q$-mode products.

Let us split radial and momentum dependence as follows:

$$V_\mu(q, r) = v_\mu(q)v(q, r), \qquad A_\mu(q, r) = a_\mu(q)a(q, r).$$
(3.43)

[We can use residual gauge symmetry to gauge-fix $q^\mu V_\mu(q, \Lambda) = q^\mu A_\mu(q, \Lambda) = 0$.] Let us also split the action of Eq. (3.42) into axial and vector parts:

$$S = S_V + S_A,$$
(3.44)

where

$$S_V = -\frac{1}{4}\int d^4q dr \frac{r^3}{\sqrt{1 + r^2\dot{T}_0^2}}V(T_0)v_\mu(q)v_\nu(-q)$$
$$\times \left(\dot{v}_q(r)\dot{v}_{-q}(r)\eta^{\mu\nu} + \frac{q^2(1 + r^2\dot{T}_0^2)}{r^4}\right.$$
$$\left. \times \left(\eta^{\mu\nu} - \frac{q^\mu q^\nu}{q^2}\right)v_q(r)v_{-q}(r)\right),$$
(3.45)

$$S_A = -\frac{1}{4}\int d^4q dr \frac{r^3}{\sqrt{1 + r^2\dot{T}_0^2}}V(T_0)a_\mu(q)a_\nu(-q)$$
$$\times \left(\dot{a}_q(r)\dot{a}_{-q}(r)\eta^{\mu\nu} + \frac{q^2(1 + r^2\dot{T}_0^2)}{r^4}\right.$$
$$\left. \times \left(\eta^{\mu\nu}\left(1 + \frac{4T_0^2 r^2}{q^2}\right) - \frac{q^\mu q^\nu}{q^2}\right)a_q(r)a_{-q}(r)\right). \quad (3.46)$$

We are interested in the transverse components of gauge fields:

$$v^T_\mu(q) = P_{\mu\lambda}\eta^{\lambda\nu}v_\nu(q), \qquad a^T_\mu(q) = P_{\mu\lambda}\eta^{\lambda\nu}a_\nu(q),$$
$$P_{\mu\nu} = \eta_{\mu\nu} - \frac{q_\mu q_\nu}{q^2},$$
(3.47)

which are described by

$$S_V^T = -\frac{1}{4} \int d^4q dr \frac{r^3}{\sqrt{1+r^2\dot{T}_0^2}} V(T_0) v_\mu^T(q) v_\nu^T(-q) \eta^{\mu\nu}$$
$$\times \left(\dot{v}_q(r)\dot{v}_{-q}(r) + \frac{q^2(1+r^2\dot{T}_0^2)}{r^4} v_q(r)v_{-q}(r) \right),$$
(3.48)

$$S_A^T = -\frac{1}{4} \int d^4q dr \frac{r^3}{\sqrt{1+r^2\dot{T}_0^2}} V(T_0) a_\mu^T(q) a_\nu^T(-q) \eta^{\mu\nu}$$
$$\times \left(\dot{a}_q(r)\dot{a}_{-q}(r) + \frac{q^2(1+r^2\dot{T}_0^2)}{r^4} \right.$$
$$\times \left. \left(1 + \frac{4T_0^2 r^2}{q^2} \right) a_q(r)a_{-q}(r) \right).$$
(3.49)

The corresponding equations of motion are

$$\ddot{v}_q(r) + \frac{\sqrt{1+r^2\dot{T}_0^2}}{r^3 V(T_0)} \frac{d}{dr} \left(\frac{r^3 V(T_0)}{\sqrt{1+r^2\dot{T}_0^2}} \right) \dot{v}_q(r)$$
$$- \frac{q^2(1+r^2\dot{T}_0^2)}{r^4} v_q(r) = 0,$$
(3.50)

$$\ddot{a}_q(r) + \frac{\sqrt{1+r^2\dot{T}_0^2}}{r^3 V(T_0)} \frac{d}{dr} \left(\frac{r^3 V(T_0)}{\sqrt{1+r^2\dot{T}_0^2}} \right) \dot{a}_q(r)$$
$$- \frac{q^2(1+r^2\dot{T}_0^2)}{r^4} \left(1 + \frac{4T_0^2 r^2}{q^2} \right) a_q(r) = 0.$$
(3.51)

We see that if there is no tachyon background, then the equations of motion for vector and axial vector fields become the same.

We must ensure that the near-horizon behavior of vector and axial vector fields is regular. The precise boundary conditions in the bulk depend strongly on the tachyon background. Below, we consider concrete tachyon potentials and determine the corresponding boundary conditions. We also require

$$v(q, r=\infty) = 1, \qquad a(q, r=\infty) = 1. \qquad (3.52)$$

We solve the equations of motion for $v(q, r)$ and $a(q, r)$ with these boundary conditions and plug the solutions into Eqs. (3.48) and (3.49). As a result, we obtain (recalling that at the boundary, the tachyon field vanishes)

$$S_V^{\text{on-shell}} = -\frac{1}{4} \int d^4q \Lambda^3 \eta^{\mu\nu} v_\mu^T(q) v_\nu^T(-q) \dot{v}(q, \Lambda), \quad (3.53)$$

$$S_A^{\text{on-shell}} = -\frac{1}{4} \int d^4q \Lambda^3 \eta^{\mu\nu} a_\mu^T(q) a_\nu^T(-q) \dot{a}(q, \Lambda). \quad (3.54)$$

Due to AdS/CFT correspondence,

$$i \int d^4x e^{iqx} \langle j_V^\mu(x) j_V^\nu(0) \rangle = \frac{\delta^2 S_V^{\text{on-shell}}}{\delta v_\mu^T(q) \delta v_\nu^T(-q)} \Bigg|_{v=0},$$
(3.55)

and similarly for the axial current. Consequently, using Eq. (3.1), we get

$$\Pi_{\mu\nu}^V = P_{\mu\nu} \Pi_V(q^2) = \frac{\delta^2 S_V^{\text{on-shell}}}{\delta v_\mu^T(q) \delta v_\nu^T(-q)}. \qquad (3.56)$$

Therefore, the correlation functions for vector and axial currents are given by

$$\Pi_V(q^2) = -\frac{1}{2} \Lambda^3 \dot{v}(q, \Lambda), \qquad (3.57)$$

$$\Pi_A(q^2) = -\frac{1}{2} \Lambda^3 \dot{a}(q, \Lambda). \qquad (3.58)$$

The propagators for vector and axial-vector currents in the field theory become the same if the tachyon background vanishes. A nonvanishing tachyon background breaks chiral symmetry, and therefore generally speaking, we have a nonvanishing S parameter, defined as

$$S = -4\pi \frac{d}{dq^2} [\Pi_V(q^2) - \Pi_A(q^2)]_{q^2=0}. \qquad (3.59)$$

With the help of holographic expressions [Eqs. (3.57) and (3.58)], we obtain

$$S = 2\pi\Lambda^3 \frac{d}{dq^2} (\dot{v}(q^2, \Lambda) - \dot{a}(q^2, \Lambda)). \qquad (3.60)$$

The infrared behavior is specific for each particular tachyon potential, and we discuss it below. Now let us consider the near-boundary region. In the near-boundary region $r \gg 1$, we can totally neglect the tachyon field, which makes the equations of motion for vector and axial-vector fields the same:

$$\ddot{v} + \frac{3}{r}\dot{v} - \frac{q^2}{r^4}v = 0, \qquad (3.61)$$

$$\ddot{a} + \frac{3}{r}\dot{a} - \frac{q^2}{r^4}a = 0. \qquad (3.62)$$

In practical computations, one has to make sure that the last term in Eq. (3.51) is small; $T_0^2 r^2/q^2 \sim (q^2 r^2)^{-1} \ll 1$ in the near-boundary region. This is important, because momentum q competes in smallness with $1/r$ when one is computing the S parameter. The cutoff is supposed to be sent to infinity first, for each value of momentum q. The solutions to these equations, normalized by the near-boundary condition [Eq. (3.52)], are

$$v = 1 - \frac{q^2}{2r^2} \log r + C_v \frac{1}{r^2}, \qquad (3.63)$$

$$a = 1 - \frac{q^2}{2r^2}\log r + C_a\frac{1}{r^2}, \qquad (3.64)$$

where $C_v(q^2)$ and $C_a(q^2)$ define asymptotic near-boundary behavior of the vector fields, have dimension 2, and go to finite constants when $q^2 = 0$. Therefore, substituting Eqs. (3.63) and (3.64) into Eq. (3.60), we find

$$S = 4\pi\frac{d}{dq^2}(C_a - C_v)|_{q^2=0}. \qquad (3.65)$$

Notice that the S parameter is expressed only via the coefficients $C_{v,a}$, describing the near-boundary behavior of vector and axial-vector gauge fields, and does not depend on the cutoff Λ.

The tachyon field describes chiral symmetry breaking at an energy scale given holographically by $r \ll \mu$. In that region, we have, essentially, different dynamics of axial vector and vector gauge fields. In what follows, we measure all dimensionful quantities in units of dynamically generated scale μ.

1. Soft wall

Consider the tachyon potential

$$V(T) = (1 + (A - 2)T^2)e^{-AT^2}, \qquad (3.66)$$

with $A > 2$. Near the horizon in this potential, the tachyon field behaves as $T_0(r) = 1/r^{A/2}$. Correspondingly, the Lagrangian for vector field fluctuation is

$$L_v = r^{3-\frac{A}{2}}e^{-\frac{A}{r^A}}\left(\dot{v}^2 + \frac{q^2A^2}{4}r^{-A-4}v^2\right). \qquad (3.67)$$

It is useful to redefine

$$v = r^{\frac{A+2}{2}}e^{\frac{A}{2r^A}}\psi_v \qquad (3.68)$$

and consider the Lagrangian for ψ_v:

$$L_v = r^{\frac{10+A}{2}}\dot{\psi}_v^2 + \frac{A^4}{4}r^{\frac{3(2-A)}{2}}\psi_v^2. \qquad (3.69)$$

The solution of the corresponding equation of motion is a linear combination of Bessel functions $I_{\pm\alpha}(\frac{A}{2r^A})$ times a power of r, of which the regular combination behaves as

$$\psi_v = r^{\frac{A}{4}-2}e^{-\frac{A}{2r^A}}. \qquad (3.70)$$

Correspondingly,

$$v = r^{\frac{3A}{4}-1}. \qquad (3.71)$$

The near-horizon Lagrangian for the axial field is

$$L_a = r^{3-\frac{A}{2}}e^{-\frac{A}{r^A}}\left(\dot{a}^2 + \frac{A^2}{r^{2(A+1)}}a^2\right). \qquad (3.72)$$

It is convenient to make a redefinition

$$a = r^{\frac{A+2}{2}}e^{\frac{A}{2r^A}}\psi_a. \qquad (3.73)$$

The near-horizon Lagrangian for the axial field is now

$$L_a = r^{\frac{10+A}{2}}\dot{\psi}_a^2 + \frac{A^2(A^2+4)}{4}r^{\frac{3(2-A)}{2}}\psi_a^2. \qquad (3.74)$$

Similarly to the case with a vector field, we choose the regular solution, which is

$$\psi_a = r^{\frac{A}{4}-2}\exp\left(-\frac{\sqrt{A^2+4}}{2r^A}\right). \qquad (3.75)$$

Correspondingly, the near-horizon behavior of the axial field is given by

$$a = r^{\frac{3A}{4}-1}\exp\left(-\frac{\sqrt{A^2+4}-A}{2r^A}\right). \qquad (3.76)$$

To summarize, we have the following near-horizon boundary conditions:

$$T_0(r) = \frac{1}{r^{A/2}}, \qquad v(r) = r^{\frac{3A}{4}-1},$$

$$a(r) = r^{\frac{3A}{4}-1}\exp\left(-\frac{\sqrt{A^2+4}-A}{2r^A}\right). \qquad (3.77)$$

We present the results of numeric evaluations of the S parameter for different values of A in Fig. 3.

2. Hard wall

Consider the hard-wall tachyon potential

$$V(T) = (\cos T)^4. \qquad (3.78)$$

The IR regime of the field theory corresponds to the near-hard-wall region of AdS space, $r \simeq \mu$, where μ is the dynamically generated scale. Let us measure all dimensional quantities in units of μ. Then the hard wall is located at $r = 1$. When $r \simeq 1$, the tachyon field behaves as
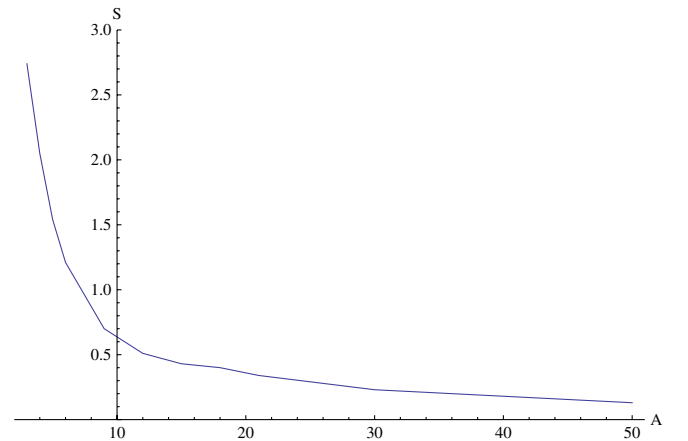

FIG. 3 (color online). S parameter in the soft-wall potential [Eq. (3.66)], depending on the value of the parameter A.

$$T(r) \simeq \frac{\pi}{2} - c\sqrt{r - 1}, \qquad c = \sqrt{\frac{5}{2}}. \qquad (3.79)$$

Plugging Eq. (3.79) into the equations of motion for vector and axial-vector gauge fields [Eqs. (3.50) and (3.51)] and considering the region near $r = 1$, we obtain

$$\ddot{v} + \frac{5}{2(r-1)}\dot{v} - \frac{5q^2}{8(r-1)}v = 0, \qquad (3.80)$$

$$\ddot{a} + \frac{5}{2(r-1)}\dot{a} - \frac{5(q^2 + \pi^2)}{8(r-1)}a = 0. \qquad (3.81)$$

The solutions are given by

$$\begin{aligned}
v &= \frac{c_1^v}{(r-1)^{1/2}}\left(1 + \frac{d_1}{r-1}\right) + c_2^v + \mathcal{O}(\sqrt{r-1}), \\
a &= \frac{c_1^a}{(r-1)^{1/2}}\left(1 + \frac{d_2}{r-1}\right) + c_2^a + \mathcal{O}(\sqrt{r-1}),
\end{aligned} \qquad (3.82)$$

where d_1 and d_2 stand for known functions of q^2. We require the momentum density T^{0r} to vanish at $r = 1$. The momentum density is given by

$$\begin{aligned}
T^{0r} &\sim \frac{1}{\sqrt{|g|}}\frac{\delta S}{\delta g_{0r}} \simeq \frac{V(T)}{\sqrt{1 + r^2\dot{T}^2}}\eta^{ij}\left[\dot{V}_i F_{0j}^{(V)} + \dot{A}_i F_{0j}^{(A)}\right] \\
&\simeq (r-1)^{5/2}(v\dot{v} + a\dot{a}). \qquad (3.83)
\end{aligned}$$

(To compute the momentum density, perturb the background metric by a small g_{0r} and keep only terms of the action which are linear in g_{0r}.)

We therefore choose the boundary conditions near the wall:

$$v = 1, \qquad a = 1. \qquad (3.84)$$

Similarly to what we have done in the soft-wall case, we can now compute the S parameter. Numerics give $S \simeq 2.6$.

IV. LIGHTEST MESONS

In this section, we compute the sigma-meson spectrum in soft-wall potential. Consider the fluctuation of the tachyon field $\tau(r, t)$ around the vacuum configuration $T_0(r)$. Expanding the TDBI action

$$S = -\int d^4x \, dr \, V(T) r^3 \left(1 + r^2(\dot{T}_0 + \dot{\tau})^2 - \frac{1}{r^2}(\partial_t\tau)^2\right)^{1/2}, \qquad (4.1)$$

we arrive at the action for the fluctuation field,

$$S = -\int d^3x \, d\omega \, dr (G(r)\dot{\tau}^2 + U(\tau)\tau^2). \qquad (4.2)$$

Perform a Fourier transform,

$$\tau(r, t) = \int \frac{d\omega}{2\pi}\tau_\omega(r)e^{i\omega\tau}, \qquad (4.3)$$

where $\omega^2 = m^2$ is the squared mass of the tachyon excitation mode. For the soft-wall potential (we consider $A > 2$ to get a discrete spectrum of sigma mesons; see Ref. [3] for details)

$$V(T) = (1 + (A - 2)T^2)e^{-AT^2}, \qquad (4.4)$$

we obtain

$$\begin{aligned}
G(r) &= 7\frac{e^{-AT_0^2}r^5(1 + (A - 2)T_0^2)}{2(1 + r^2\dot{T}_0^2)^{3/2}}, \\
U(r) &= \frac{\partial}{\partial r}\left(\frac{e^{-AT_0^2}r^5 T_0 \dot{T}_0(2 + A(A - 2)T_0^2)}{\sqrt{1 + r^2\dot{T}_0^2}}\right) \\
&+ e^{-AT_0^2}r^3(-2 + AT_0^2(10 - 3A + 2(A - 2)AT_0^2)) \\
&\times \sqrt{1 + r^2\dot{T}_0^2} - m^2\frac{e^{-AT_0^2}r(1 + (A - 2)T_0^2)}{2\sqrt{1 + r^2\dot{T}_0^2}}.
\end{aligned} \qquad (4.5)$$

Near the horizon $r = 0$, the background tachyon field behaves as $T_0 = \frac{1}{r^{A/2}}$. Therefore, the Lagrangian for the fluctuating field is

$$L = \frac{4}{A^2}r^{\frac{10+A}{2}}e^{-A/r^A}\dot{\tau}^2 - m^2 r^{\frac{2-A}{2}}e^{-A/r^A}\tau^2. \qquad (4.6)$$

It is convenient to make a redefinition $\tau = e^{A/(2r^A)}\psi$ and consider the field ψ with the Lagrangian

$$L_\psi = r^{\frac{10+A}{2}}\dot{\psi}^2 + \frac{A^4}{4}r^{\frac{3(2-A)}{2}}\psi^2. \qquad (4.7)$$

The solution of the equation of motion for the field ψ is a linear combination of Bessel functions, $I_{\pm\alpha}(A/(2r^A))$, times a power of r. We choose the regular combination of Bessel functions, which is

$$I_\alpha(A/(2r^A)) - I_{-\alpha}(A/(2r^A)) \simeq r^{A/2}e^{-A/(2r^A)}. \qquad (4.8)$$

The corresponding near-horizon behavior of the fluctuation tachyon field is

$$\tau(r) = r^{\frac{A}{4}-2}. \qquad (4.9)$$

We therefore impose the near-horizon conditions

$$\tau(\epsilon) = 1, \qquad \tau'(\epsilon) = \left(\frac{A}{4} - 2\right)\frac{1}{\epsilon}. \qquad (4.10)$$

We then integrate the equation of motion for τ with these boundary conditions up to the near-boundary region. We fit the result with the expression

$$\tau(r) = \frac{1}{r^2}(c_1 \log r + c_2). \qquad (4.11)$$

The ratio c_1/c_2 must be equal to this ratio for the background field T_0. This determines the discrete mass spectrum of tachyon excitations.
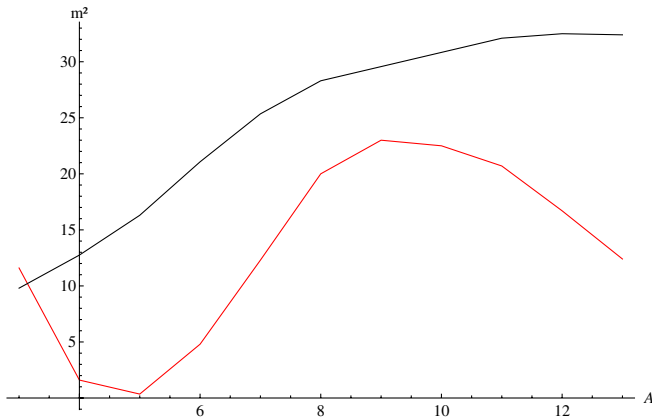
FIG. 4 (color online). The values of the masses of the first two excitations of the tachyon as a function of the parameter A of the tachyon potential [Eq. (4.4)]. The value m_1^2 (rescaled by a factor of 10) is plotted in red (lower curve), and m_2^2 is plotted in black (upper curve).

We compute numerically the values m_1^2 and m_2^2 of the masses of the first two excitations as a function of the parameter A of the tachyon potential [Eq. (4.4)]. We plot the result of these numerics in Fig. 4.

V. CONCLUSION

In this paper, we have considered strongly coupled systems which are described holographically by the tachyon DBI action in AdS space-time. These models are renormalizable: the UV cutoff can be taken to infinity while the dynamically generated mass scale stays fixed. We investigated the phase diagram of these models at finite temperature and charge density. For smaller values of temperature and chemical potential, the system resides in the phase with broken conformal symmetry. This phase is separated by a phase transition line from the phase with restored symmetry. We observe that, depending on the form of the tachyon potential, the order of the phase transition may change, and hence one or more critical points appear in the diagram. We have also used the TDBI action to describe holographically dynamical electroweak symmetry breaking. We have computed the S parameter using our holographic TDBI model for generic soft-wall tachyon potential, and for hard-wall tachyon potential. The S parameter takes generic positive values and does not appear to vanish in the parameter space that we investigated. We have also computed the masses of the lowest-lying scalar mesons and observed that even though there is no parametrically light scalar, the lightest meson can be made at least an order of magnitude lighter than the next one. Finally, it is worth noticing that the recent research of the LHC groups [55,56] indicates the experimental discovery of the Higgs boson, largely compatible with the Standard Model, and further refinements are being awaited. Also, to date, no experiment has confirmed the existence of technimesons.

APPENDIX: CONFORMAL PHASE TRANSITION AND DOUBLE-TRACE COUPLING RUNNING

Consider a gauge field theory, coupled to matter fields with a single-trace UV Lagrangian. When we go to lower energies, integrating out higher momentum modes, we generally notice [57–59] that the effective Wilsonian Lagrangian contains double-trace operators. We have to study the RG running of coupling constants for double-trace operators if we want to study the fate of the theory at low energies. Depending on the parameters defining the theory, the beta functions for double-trace operators can exhibit essentially different behavior; varying these parameters can lead to phase transitions between different IR phases of the theory. Here our focus will be on the particular type of these phase transitions, called conformal phase transitions in Ref. [60]. In this appendix, we review the field theory expectations for the physics associated with conformal phase transitions (CPT). We then use the technology of holographic Wilsonian RG to see how these expectations are reproduced in a particular holographic model based on the tachyon DBI action in AdS space.

1. Conformal phase transitions and Wilsonian RG

Consider a gauge theory with the $SU(N_c)$ gauge group, coupled to N_f massless Dirac fermions in the Veneziano limit, where both N_c and N_f are taken to infinity, with the ratio $x = N_f/N_c$ held fixed. It has a qualitatively different RG behavior depending on the value of x. Let us look at the IR effective field theory; three possible regimes can be identified. When $x > 11/2$, the theory loses asymptotic freedom and is free in the IR; when $x_c < x < 11/2$, where $x_c \simeq 4$ (see, e.g., Ref. [47]) is not known precisely, the IR theory is in the interacting Coulomb phase. This interval in x, where the theory flows to a conformal fixed point in the IR, is called the "conformal window." However, for x smaller than x_c, the IR theory acquires a mass gap and chiral symmetry is broken, due to the presence of chiral condensate.

The model studied in Ref. [59] is slightly different from the example above, but it exhibits similar behavior. The advantage is that the beta function for the double-trace operator can be computed exactly [59]. Suppose that we have some strongly interacting theory, for which all single-trace operators have vanishing beta functions; e.g., orbifold theories [61,62] or nonsupersymmetric deformations of $\mathcal{N} = 4$ super-Yang-Mills theory [63]. To see whether

the theory has conformal fixed points, we therefore have to study double-trace couplings [57–59]. Denote by $\mathcal{O}$ a single-trace operator, and consider a double-trace term in the Lagrangian, $L_{dt} = f\mathcal{O}^2$, where f is a double-trace coupling constant. In Ref. [59] (and, earlier, to the one-loop level in Refs. [57,58]) it has been shown that, depending on the parameters of the theory, the beta function for f either has a real zero (and then the theory flows to a conformal fixed point), or it does not (and then the theory generates a mass gap).

We will observe a similar behavior in the holographic model based on the tachyon DBI action in AdS space-time. First, we introduce a bulk scalar field, dual to the field theory operator $\mathcal{O}$. We choose it to be the tachyon field T, described by the tachyon DBI action. Now, we want to study renormalization of the corresponding double-trace coupling f. We will use the holographic Wilsonian renormalization as described in Ref. [64].[5] The full AdS action is written as a sum of the bulk action (in our case, it is the tachyon DBI action) defined up to the cutoff Λ, and the boundary action at $r = \Lambda$,

$$S[T] = \int_0^\Lambda dr d^d x L_0[T] + \int d^d x L_B[T]_{r=\Lambda}. \quad (A1)$$

To obtain holographically correlation functions that are invariant under the RG flow, one has to require invariance of the action S under the change of Λ: this is a holographic implementation of the Callan-Symanzik equation. The boundary term S_B encodes all degrees of freedom from the integrated-out region $r > \Lambda$ of the AdS space, and is written down as a sum of multitrace operators with corresponding coupling constants multiplying these operators. Solving for S_B, the holographic RG equation we determine the running of the dual field theory coupling constants.

Below, we apply this method to the tachyon DBI action in AdS space and find the RG behavior of the double-trace coupling f, depending on the mass m of the tachyon field. The nonvanishing tachyon field in the bulk is a preferred state when $m^2 < m_{BF}^2 = -\frac{d^2}{4}$ [3]. We conclude that f exhibits a walking behavior between the IR scale Λ_{IR} and the UV cutoff scale Λ_{UV}, which are related as $\Lambda_{IR} = \Lambda_{UV} \exp(-\frac{\pi}{\sqrt{m_{BF}^2 - m^2}})$. Such a relation confirms that our holographic model exhibits a conformal phase transition. This was also observed in Ref. [3], where a similar relation between the UV cutoff and the physical observables of the theory, such as meson masses, was established.

Finally, we remind the reader what happens as the tachyon mass squared is lowered below the Breitenlohner-Freedman bound. According to the AdS/CFT dictionary, the dimension of the operator $\mathcal{O}$, dual to the tachyon field T, is given by

---

[5]See also Ref. [65].

$$\Delta_\pm = \frac{d}{2} \pm \sqrt{\frac{d^2}{4} + m^2}. \quad (A2)$$

The two possible scaling dimensions in Eq. (A2), Δ_- and Δ_+ of the operator $\mathcal{O}$, are realized in the two conformal fixed points: the UV and IR, respectively. When we turn on a double-trace deformation $f\mathcal{O}^2$ in the UV theory, the theory flows to the IR conformal fixed point, where the dimension of $\mathcal{O}$ becomes equal to Δ_+ [66]. When the value of m^2 is lowered below $-d^2/4$, the two fixed points merge and then disappear, and the Miranski scaling emerges [2].

2. Double-trace running from tachyon DBI

Consider the tachyon DBI bulk action for the tachyon field $T(r)$ of the mass m, defined up to the UV cutoff scale $r = \Lambda$ in AdS$_{d+1}$:

$$S_0 = - \int_0^\Lambda dr \int d^d x r^{d-1} V \sqrt{1 + r^2 \dot{T}^2}, \quad (A3)$$

where tachyon potential is expanded around $T = 0$ as

$$V(T) = 1 + \frac{m^2 T^2}{2} + \cdots, \quad (A4)$$

and we denote differentiation with respect to r by the dot. Suppose we integrate out all degrees of freedom in the bulk which correspond to $r > \Lambda$. Then we generate the holographic Wilsonian effective action

$$S = S_0 + S_B[T, \Lambda], \quad (A5)$$

where S_B is the boundary term, which encodes integrated-out degrees of freedom.

The boundary condition at $r = \Lambda$ is given by

$$\Pi = \frac{\partial S_B}{\partial T}, \quad (A6)$$

where we have introduced the momentum Π, canonically conjugate to the tachyon field T:

$$\Pi = - \frac{\delta S_0}{\delta T(r = \Lambda)} = \frac{\Lambda^{d+1} V \dot{T}}{\sqrt{1 + \Lambda^2 \dot{T}^2}}. \quad (A7)$$

Using the boundary condition [Eq. (A6)], one may then express

$$\dot{T} = \frac{\partial S_B / \partial T}{\Lambda \sqrt{\Lambda^{2d} V^2 - (\partial S_B / \partial T)^2}}. \quad (A8)$$

If we denote $S_0 = \int_{r_h}^\Lambda dr \int d^d x L_0$, then the holographic RG equation is

$$\frac{\partial S_B}{\partial \Lambda} + L_0(r = \Lambda) + \frac{\partial S_B}{\partial T} \dot{T}(\Lambda) = 0. \quad (A9)$$

With the help of Eqs. (A3) and (A8), this eventually acquires the form

$$\frac{\partial S_B}{\partial \Lambda} = \Lambda^{d-1} V \sqrt{1 - \frac{1}{\Lambda^{2d} V^2}\left(\frac{\partial S_B}{\partial T}\right)^2}. \quad \text{(A10)}$$

The action S_B implicitly contains the boundary metric factor $\sqrt{-\det g_b} = \Lambda^d$. Let us make this factor explicit, defining the dimensionless boundary action $\mathcal{S}$ as

$$S_B = \Lambda^d \mathcal{S}. \quad \text{(A11)}$$

Let us also define a new cutoff coordinate,

$$\epsilon = \log\frac{\Lambda}{\mu}, \quad \text{(A12)}$$

where μ is some constant, introduced for dimensional reasons. The holographic RG equation [Eq. (A10)] therefore gets rewritten as

$$\partial_\epsilon \mathcal{S} + d\mathcal{S} = V\sqrt{1 - \left(\frac{\partial_T \mathcal{S}}{V}\right)^2}. \quad \text{(A13)}$$

Let us expand the boundary action as

$$\mathcal{S} = C(\epsilon) + J(\epsilon)T + \frac{1}{2}f(\epsilon)T^2. \quad \text{(A14)}$$

Plugging it into Eq. (A13) and matching terms of the same order in T, we obtain

$$\partial_\epsilon C = \sqrt{1 - J^2} - dC, \quad \text{(A15)}$$

$$\partial_\epsilon J = -\frac{fJ}{\sqrt{1 - J^2}} - dJ, \quad \text{(A16)}$$

$$\partial_\epsilon f = \frac{m^2}{\sqrt{1 - J^2}} - \frac{f^2}{(1 - J^2)^{3/2}} - df. \quad \text{(A17)}$$

We can solve these equations by setting $J \equiv 0$ and making $\bar{f} = -(f + d/2)$ satisfy the equation

$$\partial_\epsilon \bar{f} = \bar{f}^2 - \frac{d^2}{4} - m^2. \quad \text{(A18)}$$

Let us denote $\kappa^2 = -\frac{d^2}{4} - m^2 \equiv m_{\text{BF}}^2 - m^2$. Then, the solution to Eq. (A18) may be written as

$$\bar{f} = \kappa \tan(\kappa\epsilon). \quad \text{(A19)}$$

We conclude that double-trace coupling $\bar{f}$ exhibits a walking behavior between the UV scale

$$\Lambda_{\text{UV}} = \mu \exp\left(\frac{\pi}{2\kappa}\right) \quad \text{(A20)}$$

and the IR scale

$$\Lambda_{\text{IR}} = \mu \exp\left(-\frac{\pi}{2\kappa}\right). \quad \text{(A21)}$$

[1] B. Rosenstein, B. Warr, and S. H. Park, Phys. Rep. **205**, 59 (1991).
[2] D. B. Kaplan, J.-W. Lee, D. T. Son, and M. A. Stephanov, Phys. Rev. D **80**, 125005 (2009).
[3] D. Kutasov, J. Lin, and A. Parnachev, Nucl. Phys. **B863**, 361 (2012).
[4] D. Kutasov, J. Lin, and A. Parnachev, Nucl. Phys. **B858**, 155 (2012).
[5] M. A. Stephanov, Prog. Theor. Phys. Suppl. **153**, 139 (2004); Int. J. Mod. Phys. A **20**, 4387 (2005).
[6] R. Casalbuoni, Proc. Sci. CPOD (2006) 001.
[7] T. Alho, M. Jarvinen, K. Kajantie, E. Kiritsis, and K. Tuominen, arXiv:1210.4516.
[8] N. Evans, arXiv:1209.0626.
[9] S. R. Coleman and E. Witten, Phys. Rev. Lett. **45**, 100 (1980).
[10] M. Piai, Adv. High Energy Phys. **2010**, 464302 (2010).
[11] M. E. Peskin and T. Takeuchi, Phys. Rev. Lett. **65**, 964 (1990).
[12] M. E. Peskin and T. Takeuchi, Phys. Rev. D **46**, 381 (1992).
[13] D. C. Kennedy and B. W. Lynn, Nucl. Phys. **B322**, 1 (1989).
[14] M. E. Peskin and D. V. Schroeder, *An Introduction to Quantum Field Theory* (Addison-Wesley, Reading, MA, 1995).
[15] D. K. Hong and H.-U. Yee, Phys. Rev. D **74**, 015011 (2006).
[16] J. Hirn and V. Sanz, Phys. Rev. Lett. **97**, 121803 (2006).
[17] M. Piai, arXiv:hep-ph/0608241.
[18] C. D. Carone, J. Erlich, and J. A. Tan, Phys. Rev. D **75**, 075005 (2007).
[19] K. Agashe, C. Csaki, C. Grojean, and M. Reece, J. High Energy Phys. 12 (2007) 003.
[20] C. D. Carone, J. Erlich, and M. Sher, Phys. Rev. D **76**, 015015 (2007).
[21] R. Casalbuoni, S. De Curtis, D. Dominici, and D. Dolce, J. High Energy Phys. 08 (2007) 053.
[22] T. Hirayama and K. Yoshioka, J. High Energy Phys. 10 (2007) 002.
[23] C. D. Carone, J. Erlich, and M. Sher, Phys. Rev. D **78**, 015001 (2008).
[24] M. Fabbrichesi, M. Piai, and L. Vecchi, Phys. Rev. D **78**, 045009 (2008).
[25] F. Sannino, arXiv:0804.0182.
[26] K. Haba, S. Matsuzaki, and K. Yamawaki, Prog. Theor. Phys. **120**, 691 (2008).

[27] D. D. Dietrich and C. Kouvaris, Phys. Rev. D **78**, 055005 (2008).

[28] D. D. Dietrich and C. Kouvaris, Phys. Rev. D **79**, 075004 (2009).

[29] C. Nunez, I. Papadimitriou, and M. Piai, Int. J. Mod. Phys. A **25**, 2837 (2010).

[30] O. Mintakevich and J. Sonnenschein, J. High Energy Phys. 07 (2009) 032.

[31] H. S. Fukano and F. Sannino, Int. J. Mod. Phys. A **25**, 3911 (2010).

[32] N. Kitazawa, Int. J. Mod. Phys. A **25**, 2679 (2010).

[33] D. D. Dietrich, M. Jarvinen, and C. Kouvaris, J. High Energy Phys. 07 (2010) 023.

[34] A. V. Belitsky, Phys. Rev. D **82**, 045006 (2010).

[35] C. D. Carone and R. Primulando, Phys. Rev. D **82**, 015003 (2010).

[36] M. Reece and L.-T. Wang, J. High Energy Phys. 07 (2010) 040.

[37] K. Haba, S. Matsuzaki, and K. Yamawaki, Phys. Rev. D **82**, 055007 (2010).

[38] L. Anguelova, Nucl. Phys. **B843**, 429 (2011).

[39] M. Round, Phys. Rev. D **84**, 013012 (2011).

[40] L. Anguelova, P. Suranyi, and L. C. R. Wijewardhana, Nucl. Phys. **B852**, 39 (2011).

[41] U. I. Sondergaard, C. Pica, and F. Sannino, Phys. Rev. D **84**, 075022 (2011).

[42] D. G. Levkov, V. A. Rubakov, S. V. Troitsky, and Y. A. Zenkevich, Phys. Lett. B **716**, 350 (2012).

[43] L. Anguelova, P. Suranyi, and L. C. R. Wijewardhana, Nucl. Phys. **B862**, 671 (2012).

[44] C. D. Carone, Phys. Rev. D **86**, 055011 (2012).

[45] R. Lawrance and M. Piai, arXiv:1207.0427.

[46] D. Elander and M. Piai, arXiv:1208.0546.

[47] M. Jarvinen and E. Kiritsis, J. High Energy Phys. 03 (2012) 002.

[48] R. Alvares, N. Evans, and K.-Y. Kim, Phys. Rev. D **86**, 026008 (2012).

[49] S. Matsuzaki and K. Yamawaki, arXiv:1207.5911.

[50] N. Evans, J. French, and K.-Y. Kim, arXiv:1208.3060.

[51] S. Matsuzaki and K. Yamawaki, Phys. Rev. D **86**, 115004 (2012).

[52] Z. Chacko, R. Franceschini, and R. K. Mishra, arXiv:1209.3259.

[53] B. Bellazzini, C. Csaki, J. Hubisz, J. Serra, and J. Terning, arXiv:1209.3299.

[54] R. Casero, E. Kiritsis, and A. Paredes, Nucl. Phys. **B787**, 98 (2007).

[55] G. Aad *et al.* (ATLAS Collaboration), Phys. Lett. B **716**, 1 (2012).

[56] S. Chatrchyan *et al.* (CMS Collaboration), Phys. Lett. B **716**, 30 (2012).

[57] A. Dymarsky, I. R. Klebanov, and R. Roiban, J. High Energy Phys. 08 (2005) 011.

[58] A. Dymarsky, I. R. Klebanov, and R. Roiban, J. High Energy Phys. 11 (2005) 038.

[59] E. Pomoni and L. Rastelli, J. High Energy Phys. 04 (2009) 020.

[60] V. A. Miransky and K. Yamawaki, Phys. Rev. D **55**, 5051 (1997); **56**, 3768(E) (1997).

[61] S. Kachru and E. Silverstein, Phys. Rev. Lett. **80**, 4855 (1998).

[62] A. E. Lawrence, N. Nekrasov, and C. Vafa, Nucl. Phys. **B533**, 199 (1998).

[63] O. Lunin and J. M. Maldacena, J. High Energy Phys. 05 (2005) 033.

[64] T. Faulkner, H. Liu, and M. Rangamani, J. High Energy Phys. 08 (2011) 051.

[65] I. Heemskerk and J. Polchinski, J. High Energy Phys. 06 (2011) 031.

[66] E. Witten, arXiv:hep-th/0112258.